Journal of Marine Science and Engineering

MDPI

Article

Joint Voyage Planning and Onboard Energy Management of Hybrid Propulsion Ships

Yu Wang [1], Chengji Liang [1], Tugce Uslu Aktas [2], Jian Shi [3,*], Yang Pan [1], Sidun Fang [4] and Gino Lim [3]

[1] Institute of Logistics Science and Technology, Shanghai Maritime University, Shanghai 201306, China
[2] Department of Industrial Engineering, University of Houston, Houston, TX 77001, USA
[3] Department of Engineering Technology, University of Houston, Houston, TX 77001, USA
[4] Department of Electrical and Computer Engineering, Chongqing University, Chongqing 400044, China
* Correspondence: jshi14@uh.edu

Abstract: Maritime transportation decarbonization has become a crucial factor in reducing carbon emissions and mitigating climate change. As an industry that historically relies on fossil fuels, in particular, heavy fuel oil, the reinvention of the maritime transportation system is occurring at an unprecedented speed to integrate renewable and green energy, low-/zero- carbon fuels, and green infrastructure to support emission-free shipping. In this paper, a two-stage joint optimization model is proposed to optimize the voyage planning of a ship among multiple ports as well as its onboard energy management during each section of the voyage. More specifically, in the first stage, the arrival time of ships is optimized according to the mission of the ship and the electricity prices offered at each port. In the second stage, the speed of the ship, the dispatch of the onboard diesel engine, and the usage of energy storage systems (ESSs) are optimized based on emission control areas and maritime meteorological conditions. Simulation results have shown that the proposed approach would help ship operators minimize the operating cost over the whole voyage while significantly contributing to carbon emissions reduction.

Keywords: maritime transportation; speed optimization; navigation scheduling; electricity prices; energy management

Citation: Wang, Y.; Liang, C.; Aktas, T.U.; Shi, J.; Pan, Y.; Fang, S.; Lim, G. Joint Voyage Planning and Onboard Energy Management of Hybrid Propulsion Ships. *J. Mar. Sci. Eng.* **2023**, *11*, 585. https://doi.org/10.3390/jmse11030585

Received: 4 February 2023
Revised: 5 March 2023
Accepted: 7 March 2023
Published: 9 March 2023

1. Introduction

1.1. Background

Maritime transportation is one of the essential pillars of international transportation, moving 90% of the cross-border world trade as measured by volume [1]. Despite being considered an environmentally friendly and the least carbon-intensive mode of transport in terms of carbon dioxide (CO_2) per nautical miles transported, due to its sheer size and scale, the maritime transportation sector has been a significant greenhouse gas (GHG) emitter. According to the fourth Greenhouse Gas report of the International Maritime Organization (IMO) in 2020 [2], GHG emissions from global shipping increased by about 9.6% in 2018 compared with 2012. Without further mitigation measures, global shipping carbon emissions will rise by 40% by 2050 compared to 2018. To prevent these emissions from rising due to the increased trade demand, IMO created an initial GHG strategy in 2018 [3] to mandate that the maritime industry's GHG emissions be reduced to 40% below 2008 levels by 2030, with a long-term goal to reduce the GHG emissions by at least 50% by 2050. To support this goal, U.S. Special Presidential Envoy for Climate John Kerry pledged in April 2021 that the U.S. will work toward the IMO's GHG goal by establishing new maritime emissions reduction and efficiency requirements [4]. The European Union is planning to add the shipping industry into its cap-and-trade emission trading system as early as 2022 as a part of the EU climate law, to push the industry to move faster [5]. Meanwhile, China has also taken the initiative to cut maritime emissions by 40% before the year 2030 compared with the 2008 level, with a long-term goal of further cutting it by 70% by the year 2050. In COP 26, 22 countries signed the "Clydebank Declaration" to collectively develop at least six green shipping corridors between ports by 2025 and more before 2030 [6].

So far, various technological measures have been considered to facilitate the low-carbon evolution of the maritime transportation sector. One of the most promising technologies envisioned by the maritime community is the development and deployment of carbon-neutral fuels for ships. Currently, more than 95% of civil ships use diesel engines for propulsion [7]. Although various emission-reduction solutions have been studied in the past, such as exhaust gas recirculation or selective catalytic reduction, these techniques are still largely dependent on fossil fuels, and will hardly suffice when more and more stringent regulations and restrictions are imposed on ship emissions. As a result, the shipping sector is exploring a range of zero-emissions fuels and technologies, including batteries, biofuels, green or blue hydrogen, ammonia, and methanol, to fundamentally end the reliance on fossil fuel and remove a significant portion, if not all, of the carbon emissions [8]. For instance, the container shipping company A.P. Moller-Maersk set a 2030 interim target for a 50% reduction in emissions per transported container and has so far purchased 12 vessels using green methanol, which is produced by renewable sources such as biomass and solar energy, with the goal of upgrading a quarter of their vessel fleet to be ready for green fuels in 2030 [9]. As the world's 3rd largest container shipping company, CMA CGM has also invested in LNG as fuel as the company's first step to achieving carbon neutrality by 2050. By the end of 2021, CMA CGM had deployed six 15,000 teu LNG-powered vessels on the China–US trade [10].

Despite the apparent benefits brought by zero-emission fuels, due to ships' long lifespan, relatively fixed hull structure, and limited operating mode, powering ships with a single source of green fuels may be financially difficult, and in some cases, prohibitive. Under this context, hybrid ships have become an attractive alternative. Hybrid ships refer to ships equipped with both conventional engines that burn maritime fuel (e.g., maritime diesel) and ESS [11], such as batteries, supercapacitors [12–14], and flywheels [15–17]. Compared with conventional ships, hybrid propulsion systems provide high energy efficiency, less underwater noise, and a reduction in maintenance requirements and greenhouse gas emissions [18]. Note that for the rest of the discussion, we consider a representative hybrid ship that is powered by both diesel fuel and ESS.

As hybrid ships have the advantage of being able to switch between using conventional fuel and electrical power, when hybrid ships are docked at ports, they can connect to onshore power supplies (OPS) to supply loads and charge onboard energy storage systems (ESS) for upcoming voyages. This practice, known as cold ironing or shore power, can reduce emissions, save fuel costs, and minimize the need for maintenance on onboard generators. To effectively utilize OPS, ship operators must consider the OPS facility's availability, capacity, and electricity prices at different ports. Additionally, the ship operator needs to coordinate with the port regarding the seaside operation, such as assigning berth space and service time for loading/unloading operations. Once the ship departs from the port, onboard energy management also needs to be carefully considered, involving the alternating use of diesel engines and ESS to determine the most economical and low-emission navigation strategy, taking into account emission control areas and dynamic marine meteorological environments.

1.2. Related Works

The navigation optimization and energy management of ships have been extensively studied in the literature. For the rest of the discussion, we focus on two streams of literature: (1) voyage scheduling, including navigation mode selection and speed optimization, and (2) management of the onboard energy system.

1.2.1. Navigation Mode and Speed Optimization

The implementation of the emission control area (ECA) policy reduces the emission of polluting gases within ECA but increases the operating costs of shipping companies. Some studies highlight this issue in the literature. For instance, Zhang et al. [19] use Regression Discontinuity (RD) analysis to investigate the effectiveness of ECA policies at Shanghai Port. The experiment shows that the concentration of CO_2 in Shanghai can be significantly reduced thanks to the implementation of the ECA policy. However, this leads to an increase in the operating cost of ships and emissions of polluting gases outside ECA. Sun et al. [20] present a mixed integer linear programming model to calculate fuel consumption and select an appropriate location of ECA by collecting liner data. Li et al. [21] establish a mixed integer nonlinear programming model to obtain the optimal navigation mode and determine the avoidance strategy by analyzing the response strategy of ships to ECA. This study has found that the avoidance strategy would increase the total emissions of ships while reducing the volume of emissions within the ECA.

To cope with the increasing operation costs caused by ECA policies, several researchers have applied route selection and speed optimization to minimize these undesirable operating costs. Psaraftis et al. [22] develop a speed optimization model to provide optimal environmental benefits by considering four aspects, namely, fuel price, market state, inventory cost of cargo, and fuel consumption, depending on payload. Doudnikoff et al. [23] propose a cost model and address the problem of reducing speed within ECA to save relatively expensive fuel costs. They also consider the problem of increasing speed outside ECA to increase CO_2 emissions throughout the cycle. The results of this study indicate that the total costs may decrease, while the amount of CO_2 emissions might increase depending on the speed of the ship. Cariou et al. [24] address the idea of the European Union related to mandatory speed limits for different ship types. They argue that ships can only speed up on non-European routes once they set a speed, leading to emissions problems. Fagerholt et al. [25] consider the ECA refraction and boundary point problem. They studied ship speed optimization under strict restrictions on ships entering and leaving the ECA. Heavy fuel oil is used outside Europe, and low-sulfur fuel oil is used within Europe. Due to different fuel prices, ships have different speeds inside and outside the ECA. Wen et al. [26] present a branch-and-bound algorithm and a constraint programming model considering the benefits in terms of time, cost, and environment. They address this problem by using multiple route selection and speed optimization. Sun et al. [27] develop a collaborative optimization model considering berth and ship speed. This model could reduce port congestion and achieve the optimal ship speed with minimum fuel consumption for navigation and berthing. Zhang et al. [28] analyze the emission reduction potential of different measures and emphasize that reducing ship speed could significantly reduce carbon emissions. Fagerholt et al. [29] concentrate on the impact of ECA on shipping routes and suggest an optimization model to determine the best route and sailing speed for ships along a given port sequence. In the case of ECA, Gan et al. [30] establish a multi-objective speed optimization model by effectively compromising shipping cost and sailing time through speed optimization. They develop a ship operating cost model and voyage time model to find a Pareto solution for operating cost and voyage time. Lin et al. [31] present a mixed integer nonlinear model to maximize the revenue of shipping companies. They transform the model into a convex optimization model by variable substitution. In addition, experiments are applied to optimize speed, navigation, and cargo distribution.

While the existing literature provides useful insights into optimizing ship routing and speed considering ECA policies, operational cost, and emissions of polluting gases, most of them were designed for conventional ships that completely rely on fossil fuels. So far, the unique nature of at-berth power demand and the need of ESS charging of hybrid electric ships have not yet been adequately studied in previous research efforts. With the significant power demand from the ship to support its loading/unloading operations and to charge the onboard ESS from the shoreside, it is evident that the characteristics of the shoreside electricity system, such as electricity price, and the availability of berths with OPS equipped to serve the ship, need to be considered in the voyage planning.

1.2.2. Energy Management

For hybrid ships with ESS, energy management plays a significant role in optimizing the use of various energy sources. So far, this problem has been mainly studied in the literature with an emphasis on reducing fuel consumption, GHG emissions, and operational cost. For instance, Balestra et al. [32] develop dynamic models in Simulink, and they test different energy management strategies to optimize the most important factors in the daily operations of shipowners. Lan et al. [33] establish load variation models under five operating conditions: conventional cruise, full-speed sailing, berthing, loading and unloading, and anchoring. They propose a method to determine the optimal size of a ship's photovoltaic system, diesel generator, and energy storage system. This method aims to minimize investment costs, fuel costs, and CO_2 emissions. Planakis et al. [34] develop an energy management system and design a neural network-based speed predictor to solve the optimal power distribution problem for hybrid ship propulsion. Yi et al. [35] extend vehicle optimization techniques for hybrid ships. They simulate a dynamic programming model for a large fuel cell hybrid ship to maximize fuel cell efficiency, minimize engine fuel consumption, and keep battery SOC constant. Furthermore, Boveri et al. [36] optimized and managed the scale of the energy storage system in the power system of ships to. Fang et al. [37] offer an optimal estimation method under the constraint of a strict Energy Efficiency Operation Index (EEOI) to decide the CCS capacity of ships. The model is a two-stage programming problem. The first stage is to detect the capacity of CCS and the capacity expansion of the ESS to maintain CCS operation. The second stage is establishing a shipboard power generation and demand side joint management model to solve the power shortage caused by CCS integration. Vahabzad et al. [38] present a marine hybrid power system based on diesel generators, photovoltaic, ESS, and cold ironing equipment to meet the power needs of ships efficiently. They consider three different power sources: diesel engine, battery, and fuel cell. Wang et al. [39] consider a nested two-layer optimization structure to optimize a hybrid ship's size and energy management.

The above works have a common shortcoming in that they typically overlook the ship's mission profile when optimizing power dispatch. While this may not be a significant issue for traditional ships that rely entirely on fossil fuels, it is a critical consideration for hybrid ships because their power consumption and operation are closely tied to their voyage. Various constraints, such as whether a ship has enough at-berth time to recharge its onboard ESS, and whether it is more cost-effective to use the ESS capacity immediately or wait until the ship reaches the ECA, have a significant impact. As a result, it is apparent that energy management is not an independent issue for a multi-port and multi-stage scenario like the one described in this paper. Rather than being optimized independently, voyage scheduling and energy management must be co-optimized, which indicates that a "joint" approach is preferable.

1.3. Our Contributions

To bridge these two important gaps identified above, in this paper, we propose a two-stage joint optimization model to optimize the voyage planning of a ship among multiple ports and its onboard energy management during each section of the voyage. Considering the unique mode of energy and seaside interactions between the port and the hybrid ship, in the first stage, we aim to identify the optimal arrival and berthing arrangement of the hybrid ship to complete its mission at the lowest cost. We focus on taking into account the price of the electricity offered at different ports, in combination with the ESS demand, to help the ship determine the optimal voyage schedule. Then, the goal of the second stage is to optimize the hybrid ship's speed, the dispatch of its onboard diesel engine, and the use of its ESS based on the voyage plan derived in the first stage. Factors such as ECA and maritime weather conditions are also incorporated into the problem formulation to provide a solution that is more comprehensive and all-encompassing.

The main contributions of this paper can be summarized as follows:

(1) We aim to combine two of the most notable maritime electrification techniques—OPS and hybrid ships—to enhance the traditional scheduling practices of port operations. This integration will enable a more energy-efficient and eco-friendly maritime transportation system that leverages the benefits of both technologies. Our work is one of the pioneering efforts in this direction.
(2) We develop a two-stage optimization model to minimize the operational cost for a voyage. The first stage is optimizing the ships' arrival time depending on the electricity price. In the second stage, we optimize ship speed and ESS energy usage, taking into account various factors such as ECA conditions, maritime meteorological conditions, and the cost of different fuels.
(3) We conduct a comprehensive study to highlight how the proposed scheduling approach can effectively facilitate the voyage planning and energy interactions between the ship and shoreside OPS to improve the performance of a hybrid ship in terms of operation efficiency, electricity cost, and emission mitigation.

The rest of this article is organized as follows. In Section 2, a two-stage optimization model is proposed. In Section 3, numerical examples are implemented to test the presented model. Finally, Section 4 makes a conclusion and addresses some recommendations for future studies.

2. Model Formulation

The energy source of ships includes diesel engines and energy storage systems (ESS), which can meet service and propulsion loads. Figure 1 illustrates a representative composition of hybrid ships.

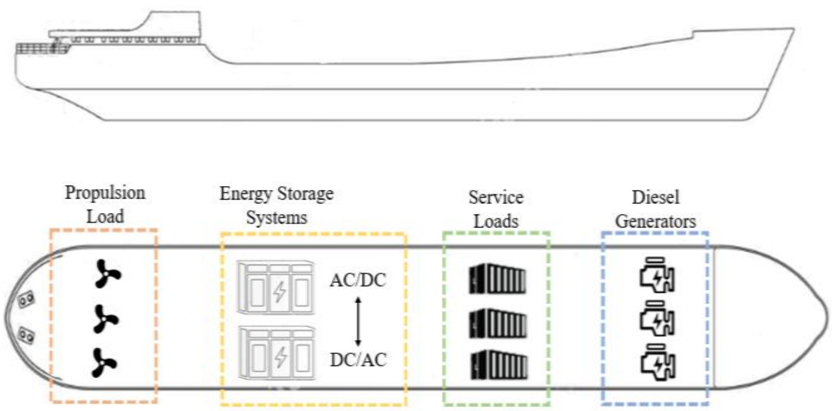

Figure 1. Hybrid ship composition.

We consider a multi-port and multi-stage problem in this paper. The multi-port problem means that ships go to various ports during their voyages, and the multi-stage problem is that ships go through multiple stages on their way from one port to another. During the voyage, ships will go through ECA. The voyage between the two ports is divided into five stages. The ships move from the port of departure to ports A, B, and C, as illustrated in Figure 2.

We propose a two-stage joint optimization model. Given the significant power demand of hybrid ships while at berth, in the first stage, we aim to optimize the voyage scheduling of a hybrid ship by minimizing the overall operation costs, including electricity consumption costs at berth that are influenced by electricity price fluctuations on the shoreside. Once the first stage is solved, the arrival time of the ships is passed to the second stage, in which we determine the speed of ships, ESS, and diesel engine energy management by minimizing the operating costs of ships and emissions released to the environment.

Figure 2. A representative illustration of a multi-port, multi-segment navigation and berthing problem.

2.1. Voyage Scheduling

When the ship is berthed, the ship uses shore power to load power to ships and charge their ESS. The price of electricity plays a crucial role in determining the arrival time of ships. Table 1 shows the parameters and variables of voyage scheduling. In the first stage, the objective function of the problem aims to minimize the cost of ship at the port, as shown in Equation (1).

$$\min \sum_{i=1}^{K} E_l(i) + E_{ch}(i) + E_{oil}(i) + E_{em}(i) \tag{1}$$

Table 1. Voyage-related variables and parameters.

Indices	
i	Ports, = 1, . . . , K
j	Stages, = 1, . . . , N
t	Stages, = time, = 1, . . . , $T_{\max}$
Parameters	
K	Number of ports
N	Number of voyage stages
$D(i,j)$	Distance to port i in stage j of the ship
$E_d(t)$	Electricity price in the t_{th} time period
F_p	Fuel prices
N_f	Fuel efficiency (kg/KWh)
$P_l(i)$	Power required to load the ship at the i_{th} port
N_{em}	Gas emission coefficient
$T_{\max}$	Maximum sailing time
$V_{\max}$	Maximum speed of ship sailing
$V_{\min}$	Minimum speed of ship sailing
Decision variables	
$\delta(i,t)$	Whether the ship arrives at the i_{th} port at time t
$V(i,j)$	Speed of the ship to the j_{th} stage of the i_{th} port

$E_l(i)$, $E_{ch}(i)$, and $E_{oil}(i)$ represent the cost of electricity for the ship's load in the i_{th} port, the cost of charging the ESS of the ship, and the cost of fuel consumption of the ship in the port, respectively. Equations (2)–(4) address $E_l(i)$, $E_{ch}(i)$, and $E_{oil}(i)$.

$E_{em}(i)$ is the emission cost of the ship at the i_{th} port. Since it is hard to compare the gas emission of ships, gas emissions are represented as emission costs. These emission costs are determined by the emission cost conversion coefficient N_{em}, as shown in Equation (5).

$$E_l(i) = E_P(i)T_{work}(i)P_l(i) \tag{2}$$

$$E_{ch}(i) = E_P(i)T_{ch}(i)N_C \tag{3}$$

$$E_{oil}(i) = \frac{P_l T_{wait}(i) F_p}{N_f} \tag{4}$$

$$E_{em}(i) = \frac{P_l T_{wait}(i) N_{em}}{N_f} \tag{5}$$

$T_{stay}(i)$ is the duration of the ship at the i_{th} port. When the ship stays in port, the power is provided to the ship's load via the shore power system. $T_{ch}(i)$ represents the charging time of ESS when the ship is at the i_{th} port. Charge time is the time from the start of charge to the end of charge for the ESS. N_C is the charging efficiency of the ship using the shore power system to charge ESS.

Equation (6) denotes the duration time of the ship at the i_{th} port, which is the sum of the waiting time of the ship arriving at the port $T_{wait}(i)$ and the berthing operation time of the ship $T_{work}(i)$. Equation (7) states the electricity price $E_P(i)$ when the ship arrives at the i_{th} port. It is obtained from the ship's arrival time and the electricity price each time.

$$T_{stay}(i) = T_{wait}(i) + T_{work}(i) \tag{6}$$

$$E_P(i) = \sum_{t=1}^{T_{\max}} \delta(i,t) E_d(t) \tag{7}$$

The ship's waiting time at the port is inversely proportional to the electricity price. In other words, the lower the electricity price, the longer the waiting time for ships. Therefore, Equation (8) arranges the waiting time of ships at the ports by electricity price.

$$T_{wait}(i) = \sum_{t=1}^{T_{\max}} \delta(i,t) \frac{N_w}{E_d(t)} \tag{8}$$

Equation (9) implies that the arrival time of ships at each port is unique.

$$\sum_{t=1}^{T_{\max}} \delta(i,t) = 1 \tag{9}$$

Equation (10) determines the arrival time of ships at i_{th} port. The arrival time of ships at the port consists of three parts. The first part indicates the time when the ship arrives at the previous port. The second part is about the berthing time of the ship in the previous port. The last part is related to the voyage time of the ship from the previous port to the current port. When the ship arrives at the first port, it only covers the sailing time from the port of departure to the first port.

$$\begin{cases} T_a(1) = \sum_{j=1}^{N} T_v(1,j) \\ T_a(i) = T_a(i-1) + T_{stay}(i-1) + \sum_{j=1}^{N} T_v(1,j) \\ i = 2,3,\ldots,Ports \end{cases} \tag{10}$$

Equation (11) determines the ship's sailing time to the i_{th} port and the j_{th} stage. The ship has a constant speed at each small stage, and sailing time is the distance of each stage divided by the speed of the current stage.

$$T_v(i,j) = \frac{D(i,j)}{V(i,j)} \tag{11}$$

The speed of the ship is within a certain range, as shown in Equation (12). Equation (13) states that the total sailing time of the ship should be less than the maximum sailing time of the ship.

$$\sum_{i=1}^{K} \sum_{j=1}^{N} T_v(i,j) + \sum_{i=1}^{K} T_{stay}(i) \le T_{\max} \tag{12}$$

$$V_{\min} \leq V(i,j) \leq V_{\max} \tag{13}$$

2.2. Energy Management

Considering ECA, dynamic marine meteorological conditions, and other factors, the speed of the ships needs to be adjusted accordingly to save the operation cost and, furthermore, since the hybrid ship is propelled by a diesel engine and ESS.

It is crucial to managing diesel engines and ESS energy. In the second stage, the operating costs of the ships during the voyage are minimized through speed optimization and energy management. Table 2 shows the parameters and variables associated with energy management.

Table 2. Energy management variables and parameters.

Parameters	
$F_p(i,j)$	Fuel price of stage j of the ship going to the i_{th} port.
C_{wind}	Coefficient of wind resistance.
C_{wave}	Coefficient of wave resistance.
C_{ts}	Coefficient of static water resistance.
$P_{e\max}$	Maximum ESS operating power.
$P_{f\max}$	Maximum operating power of diesel engine.
$Q_{e\max}$	ESS maximum energy storage.
$T_{ch}(i)$	Charging time of the ship at the i_{th} port.
ρ	Water density.
ρ_{wind}	Air density.
Variables	
$F_{\cos t}(i,j)$	Cost of the voyage of the ship to the j_{th} stage of the i_{th} port.
$P_e(i,j)$	Power of the ESS of the ship to the j_{th} stage of the i_{th} port.
$P_f(i,j)$	Power of the ship's diesel engine to the j_{th} stage of the i_{th} port.
$P_p(i,j)$	Propulsion power of the ship to the j_{th} stage of the i_{th} port.

The objective function of the second stage, which aims to minimize the fuel consumption cost at each stage during the voyage, is indicated in Equation (14).

$$\min \sum_{i=1}^{K} \sum_{j=1}^{N} F_{\cos t}(i,j) \tag{14}$$

Equation (15) is the propulsion power of a ship consisting of diesel engine power and ESS power.

$$P_p(i,j) = P_f(i,j) + P_e(i,j) \tag{15}$$

During the voyage, the ship needs to use light oil with high fuel cost to sail inside ECA, and the ships use heavy oil outside ECA. The prices of light oil and heavy oil are different. The oil price for the i_{th} port and the j_{th} stage is expressed by $F_P(i,j)$. ESS power is supplied by reserve energy due to storage size limitations, low power supply, or reserve power for subsequent stages. Therefore, in Equation (16), the cost of fuel consumption consists of two parts. One part is the fuel consumption cost generated by the diesel engine itself, and the other part is related to the cost of ESS generated by the power provided by the reserve energy. When the ESS runs out of power or conserves power for subsequent stages, the ESS is powered by reserve energy.

$$F_{\cos t}(i,j) = \frac{P_f(i,j)T_v(i,j)F_P(i,j)}{N_f} + \frac{P_e(i,j)T_{oil}(i,j)F_P(i,j)}{N_f} \tag{16}$$

$T_{oil}(i,j)$ is the voyage time of the ship using reserve energy instead of ESS in the j_{th} stage to the i_{th} port. Equation (17) ensures that the time of ESS power supply and the time of reserve energy replacing ESS power together constitute the ship's sailing time in the j_{th} stage to the i_{th} port.

$$T_{oil}(i,j) + T_e(i,j) = T_v(i,j) \tag{17}$$

As mentioned before, the ship's propulsion power at each stage is supplied by the diesel engine's power and the power of ESS. Equation (18) implies that the propulsion power of each stage is determined by the speed of the ship, maritime meteorological conditions, and other conditions.

$$P_p(i,j) = P_{wind}(i,j) + P_{wave}(i,j) + P_s(i,j) \tag{18}$$

The propulsion power of the ship is composed of three parts as follows: the power for the sailing of ships in still water, P_s, the power for overcoming wind resistance, P_{wind}, and the power for overcoming wave resistance, P_{wave}. P_s, P_{wind}, and P_{wave} are given in Equations (19)–(21).

$$P_{wind}(i,j) = \frac{C_{wind}\rho_{wind}A(V(i,j) + u_{wind}(i,j))^3}{2} \tag{19}$$

$$P_{wave}(i,j) = \frac{C_{wave}\rho g(H_{\frac{1}{3}}/2)^2 B^2(V(i,j) + u_{wave}(i,j))}{L} \tag{20}$$

$$P_s(i,j) = \frac{\rho C_{ts} S V(i,j)}{2}\left(\frac{Mn}{t_{DW}} + (1-n)\right) \tag{21}$$

When the arrival time is determined in the first stage and the berthing time is known, we can obtain the sailing time between each port. Equation (22) reflects that ships can arrive at the port with the lowest port cost as long as the sailing time between each port is guaranteed to be the same as the result of the first stage.

$$\sum_{j=1}^{N} T_v(i,j) = T_{s1}(i) \tag{22}$$

Both diesel engines and ESS are limited by the maximum power during the voyage, as mentioned in Equations (23) and (24). Equation (25) illustrates that ESS is restricted by maximum energy storage. Ships can only recharge the ESS in the ports. ESS power consumption should be at most the maximum capacity during the journey.

$$P_e(i,j) \le P_{e\max} \tag{23}$$

$$P_f(i,j) \le P_{f\max} \tag{24}$$

$$\sum_{j=1}^{N} P_e(i,j) T_e(i,j) \le Q_{e\max} \tag{25}$$

Based on the problem formulation put forward above, the first stage is a mixed integer nonlinear programming (MINLP) problem, which determines the optimal arrival time by minimizing the cost of the ship at the port. Then, the second stage is a nonlinear programming (NLP) problem that optimizes the ship's speed, the power output of the diesel engine, the power output of the ESS, and the service time of the ESS with to minimize fuel consumption costs. The flowchart for the proposed two-stage model is provided in Figure 3.

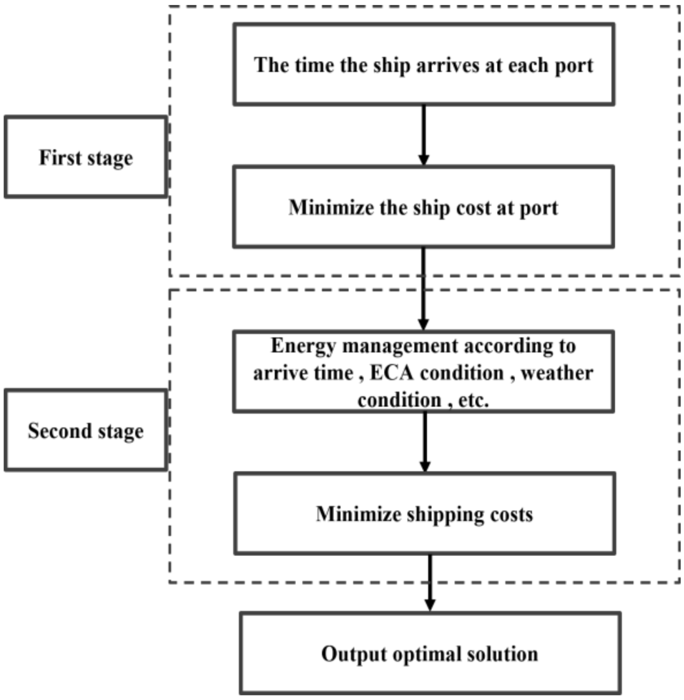

Figure 3. Flowchart of two-stage joint optimization model.

3. Numerical Analysis

The parameters of the proposed model are provided in Tables 3 and 4. Voyage parameters include voyage information and ECA boundary information. On the other hand, ship parameters include diesel engine information, ESS information, speed limit, berthing time in port, and charging time, etc. ECA selection is based on references [30,40]. Note that the data used in the experience, such as engine power, ESS capacity, and speed limitation, were modified based on [41]. We consider a single hybrid ship in the following study. Note that both stages of the proposed problem are solved by Baron in GAMS.

Table 3. Voyage parameters.

Port of Departure	Segment	ECA Inside/n Mile	ECA Outside/n Mile
A	1	50	0
	2	0	68
	3	0	55
	4	0	60
	5	40	0
B	6	40	0
	7	0	60
	8	0	87
	9	0	56
	10	45	0
C	11	45	0
	12	0	82
	13	0	63
	14	0	55
	15	40	0

Table 4. Ship parameters [40].

Ship Parameters	Numerical Value
Size of ship/m	98 × 16
Carrying capacity/ton	5000
Number of diesel engines	2
Maximum operating power of diesel engine/MWh	6
Maximum ESS operating power/MW	2
ESS maximum energy storage/MW	8
Charging efficiency	1
Load efficiency	2
Maximum sailing time /h	100
Speed limit [Min, Max]/(n mile/h)	[5, 25]
Berthing time in each port/h	[8,8,8]
Charge time for each port ESS/h	[8,8,8]

3.1. Analysis of Navigation Optimization Results

The cost of the ship in port consists of the ESS charging the cost of the ship, electricity cost of the shipload, fuel consumption cost (in the waiting area), and pollution gas emission cost of the ship. We consider different types of fuels that can be used for ships, such as Marine Gas Oil (MGO), Marine Diesel Oil (MDO), Intermediate Fuel Oil (IFO), Marine Fuel Oil (MFO) and so on. Based on the data provided in [42,43], varied fuels are priced differently, and typically, fuels that are more refined and of superior quality tend to be more expensive but result in lower emissions upon consumption. The results of the model in the first stage considering different fuel prices are shown in Table 5.

Table 5. The results of the first stage considering different fuel prices * [42,43].

Fuel Type	Fuel Price (USD)/t	Cost at Port (USD)	Fuel Cost (USD)	Emission Cost (USD)
HFO	138	1070.27	17.25	207.02
IFO180	276	1018.51	34.50	172.51
IFO380	552	1018.51	69.01	138.01
MDO	828	1018.51	103.51	103.51
MGO	1104	915.01	138.01	34.50

* Time of arrival to ports is as follows: Port A: 18; Port B: 42; Port C: 65. * Waiting time is equal to 2 for each oil price. * Price of Electricity (USD); Cost of Charging (USD); Load cost (USD) values are 8.28, 66.24, and 66.24 for each oil price, respectively.

The ship can only use fuel oil as the load drive while waiting. As shown in Figure 4, the port cost of ships rises with the increase in fuel prices. In our model, ships arrive at ports when electricity and fuel prices are low, and the waiting time for ships is longer. Although the waiting time is longer, it leads to the lowest cost of ships in ports since the oil and electricity price are also low. Therefore, when the fuel price is between $ 138 and $ 276 per ton, the ship arrives at the port when the electricity price is low and the waiting time is long.

As fuel prices increase, ships arrive at ports when electricity prices are slightly higher but waiting times are shorter. Therefore, when the fuel price is between $ 828 and $ 1104 per ton, the ship arrives at the port when the electricity price is relatively high, and the waiting time is short.

When a ship is at the port, the volume of emissions released by the ship must be considered. We convert polluting gas emissions into the corresponding pollution gas emissions cost since the amount of polluting gas emissions is difficult to measure. As discussed above, the quantity of polluting gas generated varies according to the quality of the fuel used. Fuels of superior quality, which are more expensive, generally produce lower levels of polluting emissions. Considering the pollution gas emission cost, the ship's arrival time, electricity price, waiting time of the ship, ESS charging cost, and load electricity cost are all the same, as given in Table 5. As shown in Figure 5, due to the same waiting time of ships, the fuel consumption cost of ships increases depending on the rise in fuel prices. Meanwhile, the cost of polluting gas emissions from ships decreases as fuel prices rise. Therefore, the ship's total cost at the port shows little change. When the ship uses USD 1104 per ton of fuel oil, the total cost in port is the lowest, and the environmental benefits are the highest.

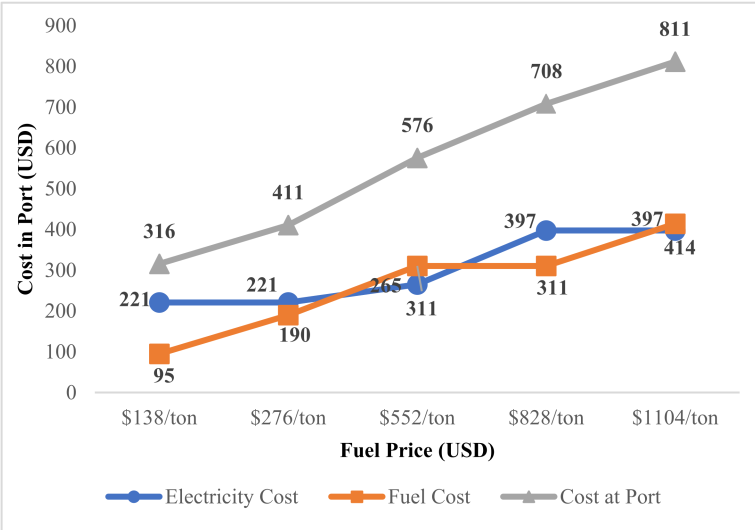

Figure 4. Cost analysis under different fuel types without considering pollution gas emission.

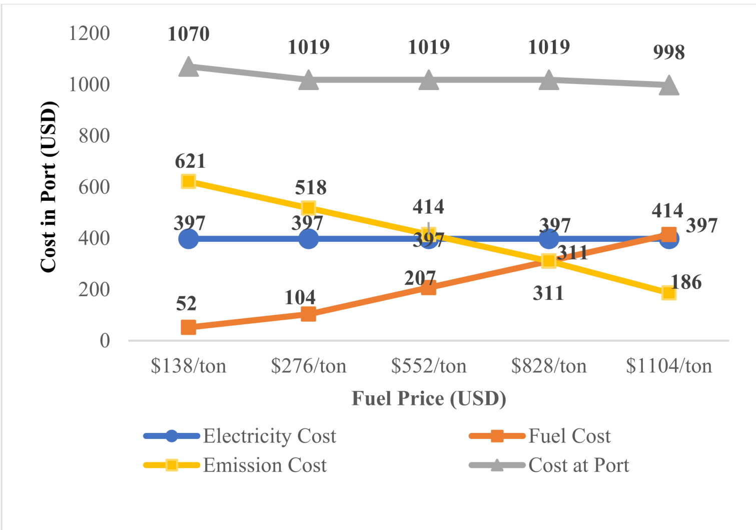

Figure 5. Cost analysis under different fuel types considering pollution gas emission.

3.2. Sensitivity Analysis of Electricity Price

Above, we analyzed the influence of different quality of fuel on the arrival time and cost of the ship in port. Next, we analyze the influence of the change in electricity price on ship navigation under the condition that the fuel price remains unchanged. When we perform the electricity price sensitivity analysis, we keep the electricity price constant from moment to moment and change the departure time of the ship. The price of electricity varies depending on the time of departure of the ship. We choose 12 a.m., 6 a.m., 12 p.m., and 6 p.m. as the departure time of the ship. We analyzed each departure time, the time it took the ship to sail to each port, the electricity price upon arrival at the port, and the cost in port.

We chose high-quality fuel with relatively high fuel prices for our analysis. As can be seen from Table 6, on the premise of using the same quality of fuel, the ships depart from different times, and the arrival time and sailing time are changed when the navigation requirements are met. The electricity price, stay time and cost in port are all the same. We can see from the table that the arrival time of ships is between 5 and 8 a.m. and between 4 and 7 p.m. The electricity price in these two periods is relatively high, but the waiting time is relatively short, so the ship's fuel consumption cost and pollution gas emission cost will be reduced. Departing at different times, the sailing time of ships may be longer or shorter, because ships choose to arrive early or late to find a time to arrive at the port at a relatively low cost.

Table 6. Sailing optimization analysis of ships with different departure times *.

	Ship Leaves at 12 a.m.		Ship Leaves at 6 a.m.		Ship Leaves at 12 p.m.		Ship Leaves at 6 p.m.	
	Time of Arrival (24 h)	Voyage Time (h)	Time of Arrival (24 h)	Voyage Time (h)	Time of Arrival (24 h)	Voyage Time (h)	Time of Arrival (24 h)	Voyage Time (h)
Port A	17	17	17	17	6	30	5	29
Port B	18	15	8	29	8	16	5	14
Port C	17	13	8	14	7	13	5	14

* The ship's choice of arrival time, electricity price, duration of stay in port, and cost in port are the same.

3.3. Analysis of Energy Management Results

Since ships can only use light oil when arriving at the port, we use the results of the model that the fuel price equals USD 1104 per ton as the constraint of the second stage. During the sailing of the ships, it is inevitable to consider ECA and maritime weather conditions. While the inside of ECA is considered in approaching the port, the outside of ECA is taken into consideration in the intermediate stage.

This paper divides each voyage into five stages. That means there are five stages between the two ports. The ECA and maritime weather conditions are the same in each sub-stage. We first consider the ECA condition. The speed and energy usage of the ship at each stage is optimized without considering the maritime weather, as shown in Table 7. As can be seen from Table 7, the speed of the ship varies among different ports due to the voyage and sailing time constraints. The speed of the ship is also different in and out of ECA. Light oil has a high oil price but low pollution, whereas heavy oil has a low oil price but high pollution. Considering only the ECA's impact on ship energy management, ships can only use light oil inside the ECA and heavy oil outside the ECA. Table 7 shows that the ship decreases the speed in ECA and uses ESS to provide power as much as possible to reduce operating costs.

Table 7. The second stage energy management results without considering the maritime weather.

Ports	Segment	ECA Inside/Outside	Speed (n mile/h)	Sailing Time (h)	Propulsion Power (MW)	Diesel Engine Power (MW)	ESS Power (MW)	ESS Service Time (h)	Reserve Service Time (h)	Fuel Costs (USD)
A	1	ECA Inside	13.84	3.61	2.54	0.65	1.90	3.61	0.00	531.75
	2	ECA Outside	17.44	3.90	5.09	5.09	0.00	0.00	0.00	2190.90
	3	ECA Outside	17.44	3.16	5.09	5.09	0.00	0.00	0.00	1772.03
	4	ECA Outside	17.44	2.44	5.09	5.09	0.00	0.00	0.00	1933.14
	5	ECA Inside	13.84	2.89	2.54	0.65	0.59	1.94	0.95	1355.11
B	6	ECA Inside	9.90	4.04	0.93	0.00	0.93	4.04	0.00	0.00
	7	ECA Outside	12.37	4.85	1.82	1.82	0.00	0.00	0.00	972.55
	8	ECA Outside	12.37	7.04	1.82	1.82	0.00	0.00	0.00	1410.18
	9	ECA Outside	12.37	4.53	1.82	1.82	0.00	0.00	0.00	907.72
	10	ECA Inside	9.90	4.55	0.93	0.00	0.93	4.55	0.00	0.00
C	11	ECA Inside	10.60	4.25	1.14	0.11	1.03	4.11	0.14	340.71
	12	ECA Outside	13.35	6.14	2.29	2.29	0.00	0.00	0.00	1291.19
	13	ECA Outside	13.35	4.72	2.29	2.29	0.00	0.00	0.00	992.01
	14	ECA Outside	13.35	4.12	2.29	2.29	0.00	0.00	0.00	866.04
	15	ECA Inside	10.60	3.78	1.14	0.11	1.07	3.53	0.24	793.56
								Total Fuel Consumption Cost:		**15,356.89**

The propulsion power of a ship consists of the diesel engine and ESS power. Ships can be powered by diesel engines, ESS, or both and must sail on light oil in the ECA. Light oil prices are higher, resulting in higher fuel consumption costs. Therefore, ship speed, diesel engine, and ESS power are optimized to reduce operating costs. However, ESS is not always available due to ESS storage limitations. When the ESS is exhausted, the ship is required to use reserve energy instead of ESS. The reserve energy needs to consume fuel oil depending on whether the ship is inside or outside ECA. As shown in Table 7, the ships go to three ports: A, B, and C. Thus, they go through three journeys, each with five stages. The first stage of the ship's journey to the first port is within the ECA. When there is no wind or waves, the propulsion power required by the ship is 2.544 MW, 0.647 MW is from the diesel engine, and 1.897 MW is from the ESS, as shown in Figure 6. The first stage of the ship's voyage takes 3.61 h. The ESS operates at 1.90 MW and the diesel engine at 0.65 MW for 3.61 h to complete the first stage of the voyage. In stages 2 to 4, the ship is outside the ECA, using heavy oil, which is cheaper. As a result, the ship's speed increases to arrive at the port on time, and operating costs are lower during the three stages. At stage 5, when the ship enters the ECA again, it needs 2.54 MW of propulsion power, 0.59 MW of ESS power, and 1.95 MW of diesel engine power. In addition, the ship needs to travel 2.89 h at that stage. Due to ESS storage limitations, ESS only provides 1.94 h of navigation. ESS requires reserve energy to provide 0.95 h running time, equivalent to increasing the fuel consumption cost of a diesel engine running 0.95 h at 0.59 MW power.

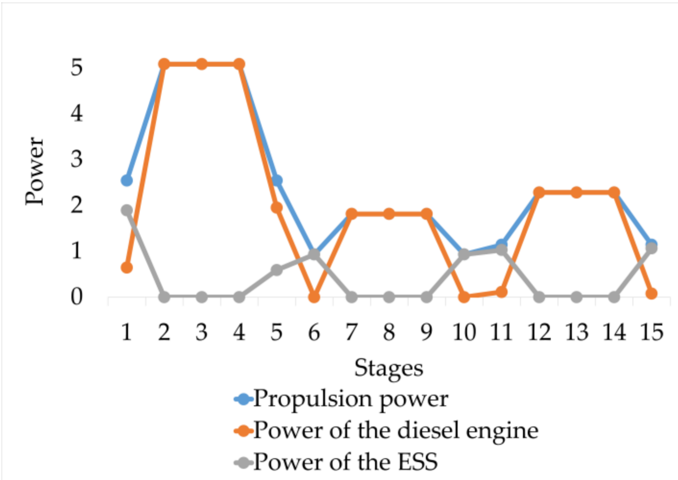

Figure 6. Comparison of propulsion power, diesel engine power, and ESS power under no wind and waves.

During the sailing, the ship will inevitably encounter wind and waves. Table 8 shows the wind and wave parameters. The second stage energy management results with increased wind and wave influence are provided in Table 9. On its way to port A, the ship encounters wind and waves in stages 2 and 3. If the ship continues to sail at the same speed, it will require more power. The results show that the ship's speed in both stages is reduced to decrease the ship's propulsion power. The propulsion power required by the ship is increased compared to the situation with no wind or waves, as illustrated in Figure 7.

Table 8. Wind speed and wave parameters.

Port of Departure	Segment	ECA Inside/Outside	Wind Speed (Knot)	Wave Speed (Knot)
A	1	ECA inside	0	0
	2	ECA outside	2	2
	3	ECA outside	3	5
	4	ECA outside	0	0
	5	ECA inside	0	0

Table 8. *Cont.*

Port of Departure	Segment	ECA Inside/Outside	Wind Speed (Knot)	Wave Speed (Knot)
B	6	ECA inside	0	0
	7	ECA outside	0	0
	8	ECA outside	5	6
	9	ECA outside	0	0
	10	ECA inside	0	0
C	11	ECA inside	0	0
	12	ECA outside	0	0
	13	ECA outside	0	0
	14	ECA outside	6	4
	15	ECA inside	0	0

Table 9. The second stage energy management results under increased wind and wave influence.

Ports	Segment	ECA Inside/Outside	Speed (n mile/h)	Sailing Time (h)	Propulsion Power (MW)	Diesel Engine Power (MW)	ESS Power (MW)	ESS Service Time (h)	Reserve Service Time (h)	Costs (USD)
A	1	ECA Inside	14.16	3.53	2.73	1.45	1.28	3.34	0.19	1181.42
	2	ECA Outside	17.01	4.00	6.80	6.00	0.80	0.00	4.00	2999.07
	3	ECA Outside	16.76	3.29	7.89	6.00	1.89	0.00	3.29	2860.80
	4	ECA Outside	17.84	3.36	5.45	5.45	0.00	0.00	0.00	2024.82
	5	ECA Inside	14.16	2.82	2.73	1.04	1.69	2.21	0.62	878.75
B	6	ECA Inside	10.18	3.93	1.01	0.02	0.99	3.86	0.07	36.27
	7	ECA Outside	12.82	4.68	2.02	2.02	0.00	0.00	0.00	1045.45
	8	ECA Outside	11.45	7.60	4.87	4.87	0.00	0.00	0.00	4087.44
	9	ECA Outside	12.82	4.37	2.02	2.02	0.00	0.00	0.00	975.77
	10	ECA Inside	10.18	4.42	1.01	0.02	0.99	4.24	0.19	63.22
C	11	ECA Inside	10.91	4.13	1.25	0.20	1.05	3.42	0.70	344.56
	12	ECA Outside	13.74	5.97	2.49	2.49	0.00	0.00	0.00	1640.75
	13	ECA Outside	13.74	4.59	2.49	2.49	0.00	0.00	0.00	1260.59
	14	ECA Outside	11.82	4.65	5.83	5.83	0.00	0.00	0.00	2996.82
	15	ECA Inside	10.91	3.67	0.03	0.03	1.21	3.65	0.02	31.77
									Total Fuel Consumption Cost:	**22,427.51**

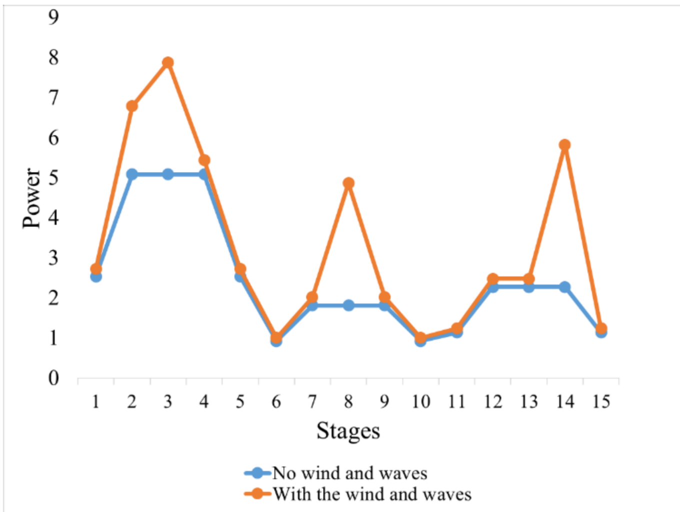

Figure 7. Comparison of propulsion power of a ship with or without wind and waves.

In the second stage, the ship encounters less wind and waves; therefore, there is less reduction in ship speed. In the third stage, the wind and waves are higher, and thus, the ship's speed is further reduced. The main reason is that the ship can only use light oil, and the ship's speed in the ECA is still low to reduce operating costs. Since the ship has low speed in the second and third stages, its speed must be increased in the first, fourth, and fifth stages to arrive at port B on time. Therefore, the ship's speed is arranged in the first, fourth, and fifth stages. Figure 8 compares the ship's speed depending on whether the ship encounters wind and waves during the voyage. The marine diesel engine has a maximum operation of 6 MW. The ship's propulsion power in the second and third stages is 6.80 MW and 7.89 MW, respectively. Diesel engines are not sufficient to provide power for the actual operations of the ship, and ESS power, therefore, is required for its operations. To save on energy costs, ESS uses more energy for stages within the ECA. Therefore, the power provided by ESS in stage 2 and stage 3 is replaced by reserve energy to meet the operation requirements. Similarly, the ship's speed is reduced in stages 8 and 14. However, the propulsion power increases, and the ship's speed in the other stages also increases to arrive at the port on time.

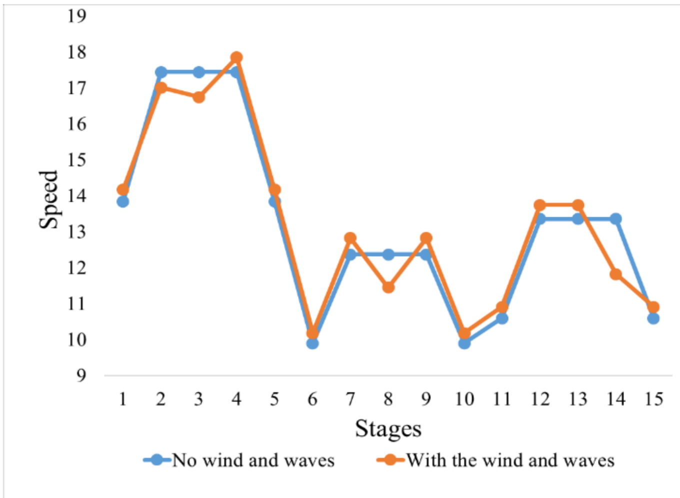

Figure 8. Speed comparison between calm and rough conditions.

3.4. Comparison of Jointed and Decouple Scheduling

Finally, we compare the performance of the proposed approach with the conventional approach that separates voyage planning and energy management. The conventional approach, which we refer to as the "decoupled scheduling approach", plans the voyage without considering the electricity price at port. Table 10 presents a comparison of the cost at port and voyage cost. For the decoupled scheduling approach, the ship's voyage time in the three sections is 18 h, 19 h, and 19 h, and the stay time in each port is 10 h, 11 h, and 10 h. In contrast, under the proposed joint scheduling approach, the ship spends 17 h, 18 h, and 17 h on the three voyages, respectively, and stays 10 h in each port. The results indicate that the proposed approach is more cost-effective, reducing the total mission cost by almost 8.8%.

Table 10. Cost comparison of jointed and decouple scheduling.

	Decoupled Scheduling	**Proposed Joint Scheduling**	**Cost Reduction**
Cost in port (USD)	1004.19	**915.01**	**8.88%**
Voyage cost (USD)	24,582.84	**22,427.51**	**8.77%**
Total cost (USD)	25,587.03	**23,342.52**	**8.77%**

4. Conclusions

This paper introduces a two-stage joint optimization model that aims to improve the navigation efficiency and energy management of hybrid ships. The first stage considers the impact of electricity prices to optimize the ship's arrival time. The second stage involves dividing the voyage into multiple parts and determining the ship's location in relation to the ECA and weather conditions, including wind and waves. The ship's speed, diesel engine, and ESS power usage are then optimized to minimize operating costs. Several important observations can be made based on the results of the simulation study: (1) The selection of the fuel plays an important role in the berthing cost of the ship, and selecting high-grade fuel may be financially beneficial for a hybrid ship considering the cost associated with emissions. (2) The onboard ESS is always exclusively reserved for use within the ECA areas, which is consistent with common practice. Under severe maritime weather conditions, the ship will lower its speed rather than use the stored energy from the ESS. (3) The performance comparison shows that, compared to the conventional scheduling approach where voyage and energy management are decoupled, the proposed joint approach can help a ship reduce the cost of completing its mission by almost 8.8%.

This research can be extended in two ways. Firstly, while the focus of this paper is on the voyage planning and energy management of a single ship, the proposed model can be extended to consider multiple ships, taking into account the potential impacts of maritime supply chains and port congestion. Secondly, the proposed model can be improved by incorporating the effects of ocean currents, resulting in a more comprehensive and well-rounded schedule solution.

Author Contributions: Y.W.: conceptualization, methodology, software, formal analysis, investigation, writing—original draft, writing—review and editing. C.L.: conceptualization, validation, investigation, resources, supervision. T.U.A.: methodology, writing—review and editing. J.S.: conceptualization, methodology, investigation, formal analysis, writing—original draft, writing—review and editing. Y.P.: writing—original draft, writing—review and editing. S.F.: conceptualization, writing—review and editing. G.L.: conceptualization, investigation, writing—review and editing, resources, supervision. All authors have read and agreed to the published version of the manuscript.

Funding: This research was funded by the National Social Science Fund of China, grant number 71972128, National Key Research and Development Plan of China, grant number 2019YFB1704403, Soft Science Research Project of Shanghai Science and Technology Innovation Action Plan, grant number 22692111200.

Institutional Review Board Statement: Not applicable.

Informed Consent Statement: Not applicable.

Data Availability Statement: The program code and data that support the plots discussed within this paper is available from the corresponding author upon request.

Acknowledgments: We are grateful to the editors and anonymous referees for their valuable comments, and detailed suggestions, which helped to improve the quality of this paper.

Conflicts of Interest: The authors declare no conflict of interest.

References

1. UNCTAD. *Review of Maritime Transport 2019*; United Nation Conference on Trade and Development: Geneva, Switzerland, 2019.
2. IMO. Fourth Greenhouse Gas Study 2020. International Maritime Organization. Available online: https://www.imo.org/en/OurWork/Environment/Pages/Fourth-IMO-Greenhouse-Gas-Study-2020.aspx (accessed on 10 January 2023).
3. IMO. Initial IMO GHG Strategy 2018. International Maritime Organization. Available online: https://www.imo.org/en/MediaCentre/HotTopics/Pages/Reducing-greenhouse-gas-emissions-from-ships.aspx (accessed on 10 January 2023).
4. Esther, W. Your Climate Change Goals May Have a Maritime Shipping Problem. Available online: https://www.spglobal.com/esg/insights/your-climate-change-goals-may-have-a-maritime-shipping-problem (accessed on 10 January 2023).
5. European Commission. Reducing Emissions from the Shipping Sector. 2021. Available online: https://ec.europa.eu/clima/eu-action/transport-emissions/reducing-emissions-shipping-sector_en (accessed on 10 January 2023).
6. United Nations Climate Change Conference UK 2021. Clydebank Declaration For Green Shipping Corridors. Available online: https://ukcop26.org/cop-26-clydebank-declaration-for-green-shipping-corridors/ (accessed on 10 January 2023).
7. Lindstad, E.; Eskeland, G.S.; Rialland, A.; Valland, A. Decarbonizing Maritime Transport: The Importance of Engine Technology and Regulations for LNG to Serve as a Transition Fuel. *Sustainability* **2020**, *12*, 8793. [CrossRef]
8. Yuan, Y.P.; Wang, J.X.; Yan, X.P.; Shen, B.Y.; Long, T. A review of multi-energy hybrid power system for ships. *Renew. Sustain. Energy Rev.* **2020**, *10*, 110081. [CrossRef]
9. Wienberg, C. Maersk Targets Bigger and Faster Cuts in Carbon Emissions. Available online: https://www.bloomberg.com/news/articles/2022-01-12/maersk-targets-bigger-and-faster-cuts-in-carbon-emissions (accessed on 10 January 2023).

10. Ermakov, A. Natural Gas in the Transition to Low-Carbon Transport Systems: Focus on Marine Bunkering and NGVs. Available online: https://iaee2022.org/files/timetable/T000103_23_1.pdf (accessed on 10 January 2023).
11. Inal, O.B.; Charpentier, J.F.; Deniz, C. Hybrid power and propulsion systems for ships: Current status and future challenges. *Renew. Sustain. Energy Rev.* **2022**, *3*, 111965. [CrossRef]
12. Khan, M.M.S.; Faruque, M.O.; Newaz, A. Fuzzy Logic Based Energy Storage Management System for MVDC Power System of All Electric Ship. *IEEE Trans. Energy Convers.* **2017**, *1*, 798–809. [CrossRef]
13. Bao, P.; Wang, W.T. Stability Improvement of Electric Ship Propulsion System Using Supercapacitor. *J. Phys. Conf. Ser.* **2021**, *9*, 012006. [CrossRef]
14. Chen, H.; Zhang, Z.H.; Guan, C.; Gao, H.B. Optimization of sizing and frequency control in battery/supercapacitor hybrid energy storage system for fuel cell ship. *Energy* **2020**, *3*, 117285. [CrossRef]
15. Hou, J.; Sun, J.; Hofmann, H. Control development and performance evaluation for battery/flywheel hybrid energy storage solutions to mitigate load fluctuations in all-electric ship propulsion systems. *Appl. Energy* **2018**, *2*, 919–930. [CrossRef]
16. Jeong, H.W.; Ha, Y.S.; Kim, Y.S.; Kim, C.H.; Yoon, K.K.; Seo, D.H. Shore power to ships and offshore plants with flywheel energy storage system. *J. Korean Soc. Mar. Eng.* **2013**, *11*, 771–777. [CrossRef]
17. Yu, Y.L.; Wang, Y.X.; Zhang, G.S.; Sun, F. Analysis of the comprehensive physical field for a new flywheel energy storage motor/generator on ships. *J. Mar. Sci. Appl.* **2012**, *11*, 134–142. [CrossRef]
18. Jelić, M.; Mrzljak, V.; Radica, G.; Račić, N. An alternative and hybrid propulsion for merchant ships: Current state and perspective. *Energy Sources Part A Recovery Util. Environ. Eff.* **2021**, *10*, 1–33. [CrossRef]
19. Zhang, Q.; Zheng, Z.Q.; Wan, Z.; Zheng, S.Y. Does emission control area policy reduce sulfur dioxides concentration in shanghai? *Transp. Res. Part D Transp. Environ.* **2020**, *3*, 102289. [CrossRef]
20. Sun, Y.L.; Yang, L.X.; Zheng, J.F. Emission control areas: More or fewer? *Transp. Res. Part D Transp. Environ.* **2020**, *7*, 102349. [CrossRef]
21. Li, L.Y.; Gao, S.X.; Yang, W.G.; Xiong, X. Ship's response strategy to emission control areas: From the perspective of sailing pattern optimization and evasion strategy selection. *Transp. Res. Part E Logist. Transp. Rev.* **2019**, *12*, 101835. [CrossRef]
22. Psaraftis, H.N.; Kontovas, C.A. Ship speed optimization: Concepts, models and combined speed-routing scenarios. *Transp. Res. Part C Emerg. Technol.* **2014**, *7*, 52–69. [CrossRef]
23. Doudnikoff, M.; Lacoste, R. Effect of a speed reduction of containerships in response to higher energy costs in sulphur emission control areas. *Transp. Res. Part D Transp. Environ.* **2014**, *5*, 19–29. [CrossRef]
24. Cariou, P.; Cheaitou, A. The effectiveness of a European speed limit versus an international bunker-levy to reduce CO_2 emissions from container shipping. *Transp. Res. Part D Transp. Environ.* **2012**, *3*, 116–123. [CrossRef]
25. Fagerholt, K.; Psaraftis, H.N. On two speed optimization problems for ships that sail in and out of emission control areas. *Transp. Res. Part D Transp. Environ.* **2015**, *8*, 56–64. [CrossRef]
26. Wen, M.; Pacino, D.; Kontovas, C.A.; Psaraftis, H.N. A multiple ship routing and speed optimization problem under time, cost and environmental objectives. *Transp. Res. Part D Transp. Environ.* **2017**, *5*, 303–321. [CrossRef]
27. Sun, B.; Niu, B.H.; Xu, H.F.; Ying, W.Z. Cooperative optimization for port and shipping line with unpredictable disturbance consideration. In Proceedings of the 2018 14th International Conference on Natural Computation, Fuzzy Systems and Knowledge Discovery (ICNC-FSKD), Huangshan, China, 28–30 July 2018; pp. 113–118.
28. Zhang, Z.; Xu, G.P.; Li, X.H.; Zhu, T.L.; Fu, P. Analysis of shipping carbon reduction measures and the scenarios of shipping carbon reduction in China. *Ind. Saf. Environ. Prot.* **2021**, *9*, 63–69.
29. Fagerholt, K.; Gausel, N.T.; Rakke, J.G.; Psaraftis, H.N. Maritime routing and speed optimization with emission control areas. *Transp. Res. Part C Emerg. Technol.* **2015**, *3*, 57–73. [CrossRef]
30. Gan, L.X.; Lu, T.F.; Zheng, Y.Z.; Shu, Y.Q. Multi-objective optimization model of ship speed control for a route passing through eca. *Navig. China* **2020**, *9*, 15–19.
31. Lin, G.H.; Gao, J.; Li, Y.W.; Xu, W.N. Optimization of liner routes and cargo allocation under eca and carbon tax policy. *Ind. Eng. Manag.* **2021**, *5*, 46–55.
32. Balestra, L.; Schjølberg, I. Energy management strategies for a zero-emission hybrid domestic ferry. *Int. J. Hydrogen Energy* **2021**, *11*, 38490–38503. [CrossRef]
33. Lan, H.; Wen, S.L.; Hong, Y.Y.; Yu, D.C.; Zhang, L.J. Optimal sizing of hybrid pv/diesel/battery in ship power system. *Appl. Energy* **2015**, *11*, 26–34. [CrossRef]
34. Planakis, N.; Papalambrou, G.; Kyrtatos, N. Predictive power-split system of hybrid ship propulsion for energy management and emissions reduction. *Control. Eng. Pract.* **2021**, *6*, 104795. [CrossRef]
35. Yi, H. Optimal operation strategy of a large fuel-cell hybrid ship. *J. Adv. Mar. Eng. Technol.* **2021**, *8*, 167–173. [CrossRef]
36. Boveri, A.; Silvestro, F.; Molinas, M.; Skjong, E. Optimal sizing of energy storage systems for shipboard applications. *IEEE Trans. Energy Convers.* **2018**, *11*, 801–811. [CrossRef]
37. Fang, S.D.; Xu, Y.; Li, Z.M.; Ding, Z.H.; Liu, L.; Wang, H.D. Optimal sizing of shipboard carbon capture system for maritime greenhouse emission control. *IEEE Trans. Ind. Appl.* **2019**, *8*, 5543–5553. [CrossRef]
38. Vahabzad, N.; Mohammadi-Ivatloo, B.; Anvari-Moghaddam, A. Optimal energy scheduling of a solar-based hybrid ship considering cold-ironing facilities. *IET Renew. Power Gener.* **2021**, *2*, 532–547. [CrossRef]

39. Wang, X.Z.; Shipurkar, U.; Haseltalab, A.; Polinder, H.; Claeys, F.; Negenborn, R.R. Sizing and control of a hybrid ship propulsion system using multi-objective double-layer optimization. *IEEE Access* **2021**, *5*, 72587–72601. [CrossRef]
40. Zhang, M.; Tan, Z.J.; Gao, P.H. Optimizing Trajectory and Speed of Coastal Ship under Irregular ECA Boundary. *J. Dalian Marit. Univ.* **2023**, *1*, 1–11.
41. Wen, S.L.; Zhao, T.Y.; Tang, Y.; Xu, Y.; Zhu, M.; Fang, S.D.; Ding, Z.H. Coordinated optimal energy management and voyage scheduling for all-electric ships based on predicted shore-side electricity price. *IEEE Trans. Ind. Appl.* **2020**, *10*, 139–148. [CrossRef]
42. Shanghai Shipping Exchange. China Shipping Exchange Network. Available online: https://www.cn-eship.com/ (accessed on 3 March 2023).
43. CNSS. China Maritime Service Network. Available online: https://www.cnss.com.cn/html/gkryjg (accessed on 3 March 2023).